Preliminary Numerical Simulation of Fluid Flow in a Helical Coil Steam Generator: A comparative study of LBM and FVM

Junyong Park [a], Minseo Lee [b], Chaehyeon Song [c], Bumjin Cho [c], Minseop Song [c], Joongoo Jeon [b*]
[a] *Department of Quantum System Engineering, Jeonbuk National University,567, Baekje-daero, Deokjin-gu, Jeonju-si, Republic of Korea*
[b] *Division of Advanced Nuclear Engineering, POSTECH, 77 Cheongam-ro, Nam-gu, Pohang-si, Gyeongsangbuk-do, Republic of Korea*
[c] *Department of Nuclear Engineering, Hanyang University, Wangsimni-ro, Seongdong-gu, Seoul, Republic of Korea*
[*] *Corresponding author: jgjeon41@postech.ac.kr*

Keywords : lattice Boltzmann method, multiple relaxation time, helical coil steam generator, finite volume method

1. Introduction

The lattice Boltzmann method (LBM) has been widely used as a powerful numerical approach for investigating complex fluid systems. From a mesoscopic perspective, LBM computes particle distribution functions and is well suited for massively parallel computing, demonstrating its effectiveness across a wide range of engineering applications. In particular, LBM has attracted attention as an efficient alternative to conventional macroscopic approaches for flows involving complex geometries and/or multiphase phenomena [1].

A helical coil steam generator (HCSG), a key component of steam generation systems, has been extensively adopted in advanced reactor concepts and compact heat-exchange systems due to its high heat-transfer capability and structural compactness. However, the strongly curved helical geometry induces significant centrifugal forces and associated secondary flows, leading to highly complex turbulent characteristics. Accurately predicting these phenomena is essential for designing the thermal performance and ensuring the safety of the system.

Traditionally, the finite volume method (FVM) has been widely employed in fluid mechanics and heat-transfer research. FVM is based on conservation laws and can handle complex geometries using unstructured meshes [2]. Nevertheless, generating high-quality unstructured meshes for highly curved geometries such as HCSGs is time-consuming and labor-intensive, and the computational cost can increase substantially for high-Reynolds-number turbulent-flow simulations [3].

In contrast, LBM is characterized by its use of regular Cartesian grids, effectively eliminating the need for the complex and time-consuming mesh generation process required by conventional body-fitted methods [4]. Moreover, the multiple-relaxation-time (MRT) formulation adopted in this study offers improved numerical stability compared with the single-relaxation-time (SRT) model. When coupled with the shear stress transport (SST) k - ω turbulence model, it can capture flow separation and turbulent features in high-Reynolds-number flows with enhanced fidelity. Beyond these algorithmic advantages, LBM is inherently optimized for massively parallel acceleration on Graphics Processing Units (GPUs) due to its localized collision and streaming operations, which maximize memory bandwidth utilization.

However, as the Reynolds number increases, capturing the fine structures of intense turbulence requires an extremely high spatial resolution within the computational domain. This leads to a substantial increase in the total number of computational operations, resulting in significant costs despite the benefits of GPU acceleration. To overcome this limitation, just as Artificial Intelligence (AI) is hybridized with mesh-based methods like FVM in a Residual-based Physics-Informed Transfer Learning (RePIT) strategy, LBM frameworks—which similarly eliminate complex mesh generation—can be coupled with various AI accelerators to achieve high-fidelity data with significantly reduced computational overhead. Therefore, the objective of this study is to apply an MRT-LBM framework to the flow analysis of an HCSG and to validate its numerical accuracy and computational efficiency by comparison with benchmark FVM simulation data. By establishing this high-fidelity numerical foundation, this work not only evaluates the performance of LBM for complex geometries but also provides the essential validation datasets required for the future development of an AI-LBM hybrid solver integrated with RePIT to ensure its physical reliability.

2. Numerical Modeling

This section details the numerical methodologies and computational frameworks employed to investigate the turbulent flow characteristics within the HCSG. The mathematical formulation of the LBM with a MRT collision scheme is first established, followed by the description of the SST $k-\omega$ turbulence model integration. Additionally, the numerical setups for the FVM, which serves as the benchmark for validation, are presented to provide a comprehensive basis for comparative analysis.

2.1 Lattice Boltzmann Method

The LBM is a mesoscopic approach that describes fluid flow by evolving particle distribution functions on a discretized lattice, rooted in kinetic theory. Unlike traditional CFD methods that numerically solve the macroscopic Navier-Stokes equations directly, LBM recovers fluid behavior through a repetitive sequence of collision and streaming operations.

The fundamental evolution of the LBM is governed by the discrete-velocity Boltzmann equation, where the unknown particle distribution function $f_\alpha(x,t)$ is updated as follows:

$$f_\alpha(x + e_\alpha \Delta t, t + \Delta t) = f_\alpha(x,t) + \Omega_\alpha(f) \quad (1)$$

In Eq. (1), α represents the discrete lattice velocities and Ω_α denotes the collision operator accounting for particle interactions. This process represents a relaxation toward an equilibrium state while conserving mass and momentum.

Through the Chapman-Enskog expansion, it can be mathematically demonstrated that the LBM recovers the standard incompressible Navier-Stokes equations in the limit of a small Mach number. This theoretical framework ensures that the mesoscopic interactions on the lattice effectively represent the macroscopic physics of the fluid flow [5].

2.1.1 Lattice Model

In this study, the D2Q9 (two-dimensional, nine-velocity) model is employed for the efficient discretization of the flow field. This model is characterized by a square lattice where particles are either at rest at the center (index 0) or move toward eight neighboring nodes.

The discrete velocity vectors, e_α, for the D2Q9 model are defined in Eq. (2) and their directions are illustrated in Fig. 1.

$$e_\alpha = \begin{cases} (0,0) & \alpha = 0 \\ (cos\theta_\alpha, sin\theta_\alpha)c\,, \theta_\alpha = \dfrac{(\alpha-1)\pi}{2} & \alpha = 1,2,3,4 \\ (cos\theta_\alpha, sin\theta_\alpha)\sqrt{2}c\,, \theta_\alpha = \dfrac{(\alpha-5)\pi}{2} + \dfrac{\pi}{4} & \alpha = 5,6,7,8 \end{cases} \quad (2)$$

where $c = \Delta x/\Delta t$ represents the lattice speed. To ensure the isotropy of the fluid and accurately recover the macroscopic Navier-Stokes equations, the weight factors ω_i are assigned to each direction as specified in Eq. (3):

$$\omega_\alpha = \begin{cases} 4/9 & \alpha = 0 \\ 1/9 & \alpha = 1,2,3,4 \\ 1/36 & \alpha = 5,6,7,8 \end{cases} \quad (3)$$

These weight factors from Eq. (3) and discrete velocities defined in Eq. (2) satisfy essential moment properties, such as $\sum \omega_\alpha = 1$ and $\sum \omega_\alpha\, e_{\alpha,i} e_{\alpha,j} = \frac{c^2}{3}\delta_{ij}$, which provide the physical foundation for the LBM numerical framework [6].

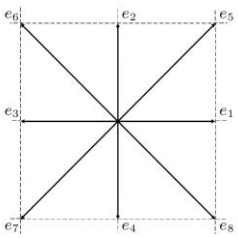

Fig. 1. Discrete velocity directions and configuration of the D2Q9 lattice model.

2.1.2 Collision Operator

The collision process in the LBM is traditionally modeled using the SRT approximation, also known as the lattice Bhatnagar-Gross-Krook (LBGK) model. However, the SRT model often suffers from numerical instabilities at high Reynolds numbers and is limited by a fixed Prandtl number. To overcome these deficiencies, this study employs the MRT collision operator, which offers superior numerical stability and flexibility by relaxing different physical moments at different rates [7].

The evolution equation for the MRT-LBM is expressed in the moment space as follows in Eq. (4):

$$f_\alpha(x + e_\alpha \Delta t, t + \Delta t) - f_\alpha(x,t) = -M^{-1} S [m_\alpha(x,t) - m_\alpha^{eq}(x,t)] \quad (4)$$

$$\boldsymbol{M} = \begin{bmatrix} 1 & 1 & 1 & 1 & 1 & 1 & 1 & 1 & 1 \\ -4 & -1 & -1 & -1 & -1 & 2 & 2 & 2 & 2 \\ 4 & -2 & -2 & -2 & -2 & 1 & 1 & 1 & 1 \\ 0 & 1 & 0 & -1 & 0 & 1 & -1 & -1 & 1 \\ 0 & -2 & 0 & 2 & 0 & 1 & -1 & -1 & 1 \\ 0 & 0 & 1 & 0 & -1 & 1 & 1 & -1 & -1 \\ 0 & 0 & -2 & 0 & 2 & 1 & 1 & -1 & -1 \\ 0 & 1 & -1 & 1 & -1 & 0 & 0 & 0 & 0 \\ 0 & 0 & 0 & 0 & 0 & 1 & -1 & 1 & -1 \end{bmatrix}$$

Fig. 2. The transformation matrix M for the D2Q9 model [6].

where **M** is a transformation matrix illustrated in Fig. 2, that maps the distribution functions f_α to their corresponding moments m_α (m = **M***f*), and **S** is a diagonal relaxation matrix **[7]**. The relaxation matrix **S** contains the relaxation rates s_i for each moment, allowing for independent control over bulk and shear viscosities.

According to the Chapman-Enskog expansion, the kinematic viscosity ν in the macroscopic limit is related to the relaxation time of the momentum-flux moments as follows in Eq. (5):

$$\nu = c_s^2 \left(\tau - \frac{1}{2}\right)\Delta t = \frac{1}{3}\left(\frac{1}{s_i} - \frac{1}{2}\right)\Delta t \quad (5)$$

where $c_s = 1/\sqrt{3}$ is the lattice speed of sound. By carefully tuning the relaxation parameters in the MRT framework, the numerical simulation can accurately recover the incompressible Navier-Stokes equations even under the complex turbulent conditions found in a helical coil steam generator.

2.2 Computational Domain and Geometry

The computational domain in this study represents a staggered-array configuration of a HCSG. Geometry (staggered-array) consists of a radial direction of 252 mm, an axial direction of 94 mm, a tube diameter of 12 mm, and pitches of 13.5 mm and 18.29 mm. This specific arrangement is designed to analyze the complex turbulent flow characteristics within the tube bundle. The schematic representation of the modeled geometry is illustrated in Fig. 3.

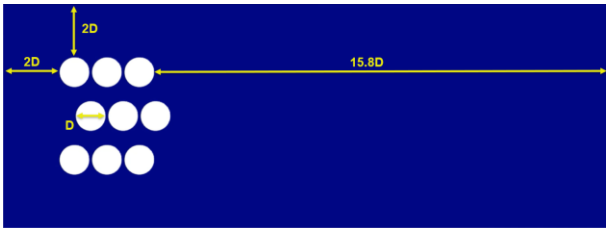

Fig. 3. Domain of Geometry

2.3 Turbulence Modeling

To accurately capture complex flow separation and turbulent behavior around the helical coil structures, Menter's SST k - ω model was employed [8]. This hybrid approach utilizes the k - ω model in the near-wall region and transitions to the k - ϵ model in the far-field, offering superior performance in predicting flow separation under adverse pressure gradients [8].

Within the LBM framework, the turbulence kinetic energy (k) and the specific dissipation rate (ω) are solved through coupled Advection-Diffusion Equations (ADE). The eddy viscosity, v_t, is determined by Eq. (6) [8]:

$$v_t = \frac{a_1 k}{\max(a_1 \omega, SF_2)} \tag{6}$$

where S denotes the invariant measure of the strain rate, and F_2 is a blending function based on the wall distance. The computed eddy viscosity is combined with the molecular viscosity (v_{lam}) to yield the effective viscosity (v_{eff}), which locally updates the relaxation rates (s_i) in the MRT collision operator to represent macroscopic turbulent effects.

Furthermore, an Automatic Wall Function (AWF) is implemented to enhance numerical stability and overcome resolution constraints near the solid boundaries. This method adaptively calculates the ω boundary condition based on the local y^+ value, effectively bridging the viscous sublayer and the log-law region. This ensures physically consistent predictions of wall friction and flow separation across the complex tube bundle geometry, even with limited lattice resolution.

2.4 Implementation of Boundary Conditions

In this study, specific boundary conditions were implemented to ensure numerical stability and physical accuracy. A velocity inlet boundary condition was applied at the inlet to prescribe a uniform flow speed (U_{in}), while a pressure outlet was set at the exit to allow for natural flow discharge. These conditions utilize the Zou-He method to maintain mass and momentum conservation at the boundaries. For the turbulence variables (k, ω), fixed values were assigned at the inlet via Dirichlet conditions, and a zero-gradient Neumann condition was applied at the outlet to prevent numerical reflections.

To represent the no-slip condition at the tube surfaces and domain walls, the half-way bounce-back scheme was employed. Additionally, an automatic wall function was integrated to adaptively calculate the specific dissipation rate (ω) based on the local y^+ value. This treatment effectively bridges the viscous sublayer and the outer turbulent region, enabling accurate predictions of wall friction and flow separation even at a relatively coarse lattice resolution.

2.5 Finite Volume Method Setup

To ensure the physical validity and convergence reliability of the LBM simulation, the numerical configurations were directly mapped from a pre-validated FVM setup developed in ANSYS Fluent. This approach allows for a rigorous direct comparison between the two numerical frameworks by maintaining equivalent flow conditions.

The working fluid was defined as water, with a density of 998.2 kg/m³ and a dynamic viscosity of 0.001 Pa·s. The inlet velocity was prescribed at 0.1 m/s. Based on the channel height (H = 94 mm) as the characteristic length, the Reynolds number (Re_H) was established at 9,383, serving as the primary non-dimensional parameter maintained across both the FVM and LBM simulations.

The SST k - ω turbulence model and the Production Limiter option, which were utilized in the FVM setup, were identically implemented within the turbulence closure logic of the LBM. To replicate the numerical resolution provided by the FVM's SIMPLE algorithm and second-order upwind spatial discretization, the LBM lattice resolution and relaxation parameters were carefully calibrated. Furthermore, the time advancement strategy was aligned with the FVM's adaptive time-stepping (Courant number = 1.0). This synchronization ensured that the LBM simulation achieved stable convergence over a total flow time of 10 s, capturing physically meaningful turbulent characteristics.

2.6 Results

In this study, the numerical integrity of the proposed MRT-LBM framework was evaluated by verifying its adherence to physical conservation laws and the incompressibility constraint [7]. As illustrated in Fig. 4 (a), the inlet and outlet mass flow rates reached a stable balance as the flow converged after the initial transient period. The relative mass change was maintained at an extremely low level—less than 0.3% [4]—confirming that the lattice resolution and boundary conditions employed in this work effectively satisfy mass conservation.

Regarding momentum conservation, the static pressure drop ($\Delta \boldsymbol{P}$) across the HCSG and the local velocity fluctuation data were analyzed, as shown in Fig. 4 (b). The stable oscillations of pressure and velocity with a consistent periodicity demonstrate that the model accurately captures the unsteady flow characteristics, such as vortex shedding, occurring behind the complex geometry.

Furthermore, the incompressibility constraint, which supports the theoretical validity of the LBM [5], was examined through Fig. 4 (c). The maximum Mach number ($\boldsymbol{Ma_{max}}$) measured during the simulation was approximately 0.15, which is well below the theoretical limit of 0.3 required for valid incompressible flow modeling in LBM [1, 4]. Additionally, the relative density fluctuation ($\boldsymbol{\Delta\rho/\rho}$) shown in Fig. 4 (c) remained under 1.6%, confirming that the current model numerically implements the incompressibility assumption of actual physical phenomena with high fidelity.

To further enhance the reliability of these results, future studies should include a grid convergence test for solution independence and an additional analysis of stability limits in higher Reynolds number regimes.

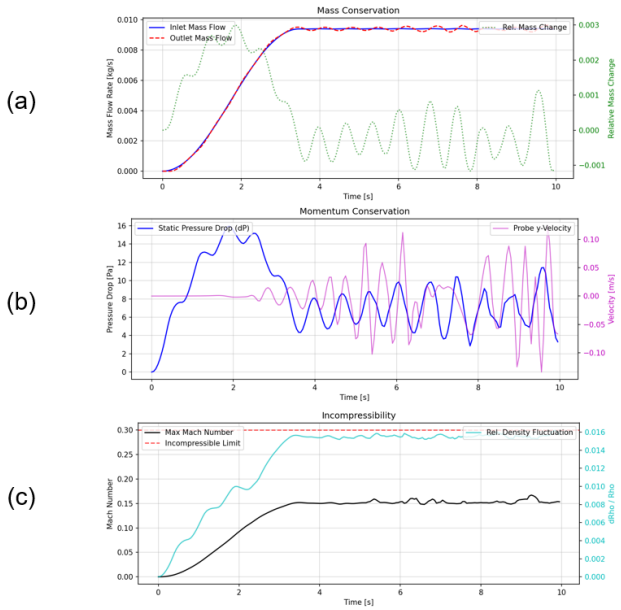

Fig. 4. Numerical validation of the LBM solver: (a) mass conservation (mass flow rates and relative change), (b) momentum conservation (pressure drop and velocity monitoring), and (c) incompressibility (Mach number and density fluctuation).

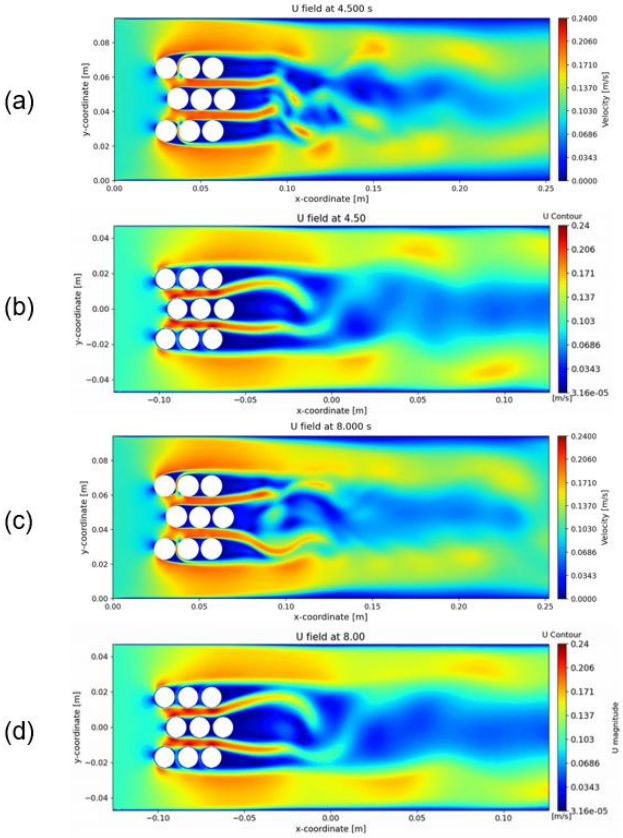

Fig. 5. Comparison of velocity magnitude contours between LBM and FVM at different flow times: (a) LBM at t = 4.5 s, (b) FVM at t = 4.5 s, (c) LBM at t = 8.0 s, and (d) FVM at t = 8.0 s.

To further evaluate the spatial accuracy of the proposed model, a qualitative comparison of velocity fields between the MRT-LBM and conventional FVM was performed [1, 3]. Fig. 5 presents the velocity magnitude contours at two distinct flow times for a direct comparative assessment. Fig. 5 (a) and (b) compare the results at the early flow stage (t = 4.50 s), while Fig. 5 (c) and (d) illustrate the comparison during the fully developed flow stage (t = 8.00 s).

At t = 4.50 s (Fig. 5 (a) and (b)), the LBM results exhibit high-velocity streams between the tube bundles and the formation of complex vortex patterns that are remarkably similar to the FVM benchmarks. Specifically, the separation points on the tube surfaces and the initial development of the wake regions show excellent visual agreement between the two numerical methods.

As the flow progresses to t = 8.00 s (Fig. 5 (c) and (d)), the LBM continues to robustly capture the increasingly complex, unsteady flow structures. The periodic vortex shedding behavior observed in the downstream region of the tubes maintains strong consistency with the FVM data. This indicates that the MRT-LBM, integrated with the SST k - ω model and automatic wall functions [8], reliably resolves the transient turbulent dynamics induced by the complex HCSG geometry across different temporal scales.

Numerical Method	***LBM***	***FVM***
Implementation Platform	GPU-accelerated (CUDA)	CPU-based Parallelization (MPI)
Computing Architecture	NVIDIA A100-SXM4-40GB	AMD EPYC 9554 (16 cores utilized)
Simulation Time	462 s	~ 1800 s

Table 1. Comparison of computational resources and simulation performance between FVM and LBM.

To provide a quantitative comparison of computational efficiency, the execution times of the two methods were measured as shown in Table 1. The FVM simulations were performed on a high-performance server equipped with AMD EPYC 9554 processors (128 cores in total), with 16 cores allocated for the computation. In contrast, the LBM framework was executed on a single NVIDIA A100-SXM4-40GB GPU. The total simulation time for the LBM was 462 s, compared to 1,800 s for the FVM. This result indicates that the LBM approach provides a significant reduction in computational turnaround time for HCSG flow analysis, achieving approximately a 3.9-fold speedup in this study.

In conclusion, the high degree of correlation between the LBM and FVM results confirms that the proposed framework achieves spatial accuracy comparable to conventional macroscopic solvers. Furthermore, the quantitative performance analysis demonstrates that the LBM effectively addresses the computational cost issues of FVM approaches by significantly enhancing simulation efficiency. These findings suggest that the proposed GPU-accelerated LBM framework is a robust and highly efficient alternative for the high-fidelity numerical analysis of complex fluid systems like HCSGs.

3. Conclusions

In this study, an MRT-LBM framework integrated with the SST k - ω turbulence model and automatic wall functions was developed and validated for the analysis of complex turbulent flows within a HCSG.

First, the numerical integrity of the solver was confirmed through physical conservation laws; the relative mass change remained below 0.3%, and the incompressibility constraint was strictly satisfied with a maximum Mach number of 0.15. These results demonstrate that the proposed framework reliably adheres to fundamental fluid dynamics principles even in complex internal geometries.

Second, the spatial accuracy of the model was qualitatively verified by comparing velocity magnitude contours with FVM benchmark data. The MRT-LBM successfully reproduced intricate flow features, such as high-velocity streams between tube bundles and unsteady vortex shedding patterns, exhibiting high fidelity to conventional macroscopic results. This close agreement across multiple time steps indicates that the model reliably captures the transient turbulent dynamics induced by the complex tube array.

In conclusion, the proposed framework provides a robust, accurate, and computationally efficient alternative to conventional CFD methods for simulating transient turbulent dynamics. Quantitative performance analysis demonstrated that the LBM on an NVIDIA A100 GPU achieved a 3.9-fold speedup in simulation runtime compared to the FVM using 16 allocated CPU cores. By significantly reducing both the pre-processing burden of complex mesh generation and the overall computational cost, this approach offers a practical advantage for industrial HCSG design. Future work will focus on performing comprehensive grid convergence tests and extending the analysis to higher Reynolds number regimes to further enhance the reliability and applicability of the framework in large-scale engineering systems.

Acknowledgments

This work was supported by the National Research Foundation of Korea (NRF) grant funded by the Korea government (MIST) (RS-2025 02634798) and by the National Research Council of Science & Technology (NST) grant by the Korea government (MIST) (No. GTL24031-000)

REFERENCES

[1] Aizat Abas, MHH Ishak, M. Z. Abdullah, "Comparative Studies of Lattice Boltzmann and Finite Volume Methods on 3D Cavity Problem," Journal of Scientific Research and Development, 2015.

[2] Z. Zhang and X. Zhang, "Direct simulation of low-re flow around a square cylinder by numerical manifold method for Navier-Stokes equations," 2012.

[3] S. Boivin, F. Cayre, and J. Herard, "A finite volume method to solve the Navier-Stokes equations for incompressible flows on unstructured meshes," 2000.

[4] A. A. Mohamad, "Lattice Boltzmann Method: Fundamentals and Engineering Applications with Computer Codes," 2011.

[5] J. Li, "Appendix: Chapman-Enskog Expansion in the Lattice Boltzmann Method," arXiv preprint arXiv:1512.02599, 2015.

[6] R. Kompová, "Acceleration of Lattice-Boltzmann Algorithms for Bloodflow Modeling," Master's thesis, Brno University of Technology, 2016.

[7] D. d'Humières, I. Ginzburg, M. Krafczyk, P. Lallemand, and L.-S. Luo, "Multiple-relaxation-time Lattice Boltzmann Models in Three Dimensions," Philosophical Transactions of the Royal Society of London. Series A: Mathematical, Physical and Engineering Sciences, vol. 360, no. 1792, pp. 437–451, 2002.

[8] F. R. Menter, "Two-equation eddy-viscosity turbulence models for engineering applications," *AIAA Journal*, vol. 32, no. 8, pp. 1598-1605, 1994.

[9] P. Lallemand and L. S. Luo, "Theory of the lattice Boltzmann method: Dispersion, dissipation, isotropy, Galilean invariance, and stability," *Physical Review E*, 2000.
[10] S. B. Pope, "Turbulent Flows," *Cambridge University Press*, 2000.